Zygote **8** (November), pp 285–293. © 2000 Cambridge University Press Printed in the United Kingdom

Meiosis-associated calcium waves in ascidian oocytes are correlated with the position of the male centrosome

Martin Wilding[1], *Marcella Marino*[2], *Vincenzo Monfrecola*[2] *and Brian Dale*[3]
Università degli Studi 'Federico II', Naples, Stazione Zoologica 'Anton Dohrn', Naples and Centre for Reproductive Biology, Naples, Italy

Date submitted: 9.12.99. Date accepted: 14.2.00

Summary

We have used confocal microscopy to measure calcium waves and examine the distribution of tubulin in oocytes of the ascidian *Ciona intestinalis* during meiosis. We show that the fertilisation calcium wave in these oocytes originates in the vegetal pole. The sperm penetration site and female meiotic apparatus are found at opposite poles of the oocyte at fertilisation, confirming that *C. intestinalis* sperm enter in the vegetal pole of the oocyte. Following fertilisation, ascidian oocytes are characterised by repetitive calcium waves. Meiosis I-associated waves originate at the vegetal pole of the oocyte, and travel towards the animal pole. In contrast, the calcium waves during meiosis II initiate at the oocyte equator, and cross the oocyte cytoplasm perpendicular to the point of emission of the polar body. Immunolocalisation of tubulin during meiosis II reveals that the male centrosome is also located between animal and vegetal poles prior to initiation of the meiosis II-associated calcium waves, suggesting that the male centrosome influences the origin of these calcium transients. Ascidians are also characterised by an increase in sensitivity to intracellular calcium release after fertilisation. We show that this is not simply an effect of oocyte activation. The data strongly suggest a role for the male centrosome in controlling the mechanism and localisation of post-fertilisation intracellular calcium waves.

Key words: Calcium induced calcium release, Centrosome, Fertilisation, IP_3, Ratiometric calcium imaging

Introduction

An increase in intracellular calcium ions accompanies fertilisation in all species of animal studied to date (Jaffe, 1980; Whitaker & Swann, 1993). This increase occurs through the release of calcium stored in organelles in the oocyte cytoplasm (Whitaker & Swann, 1993). The release of intracellular calcium is triggered through the introduction of soluble factors contained within the sperm cytoplasm into the oocyte (Dale *et al*., 1985; for review see Whitaker & Swann, 1993; Dale *et al*., 1999).

In ascidian oocytes, repetitive calcium increases follow the initial calcium wave at fertilisation (Speknijder *et al*., 1989; McDougall & Sardet, 1995; Russo *et al*., 1996; Yoshida *et al*., 1998). These have been demonstrated to occur as waves that relocalise together with the reorganisation of the ascidian oocyte cytoplasm (Rogers *et al*., 1995; McDougall & Sardet, 1995). These data suggest that a cortical pacemaker is responsible for the initiation of the post-fertilisation calcium waves (Speksnijder, 1992).

Apart from the activation of the oocyte by sperm-introduced factors, the sperm introduces its centrosome into the oocyte (Wilson & Matthews, 1895; Sluder & Reider, 1985). In most animals, the male centrosome is required for mitosis and therefore continued devel-

All correspondence to: Dr Martin Wilding. Dipartimento Clinica di Emergenza Ginecologica & Ostetrica e Medicina della Riproduzione, Azienda Universitaria Policlinico, Università degli Studi 'Federico II', Via S. Pansini, 5, 80131 Naples, Italy. Tel/fax: +39 081 7462699. e-mail: cocco.lone@libero.it
[1]Dipartimento Clinica di Emergenza Ginecologica e Ostetrica e Medicina della Riproduzione, Azienda Universitaria Policlinico, Università degli Studi 'Federico II', Naples, Italy.
[2]Stazione Zoologica 'Anton Dohrn', Villa Comunale, 1, 80121 Naples, Italy.
[3]Centre for Reproductive Biology, Clinica Villa Del Sole, Via Manzoni, 15, 80123 Naples, Italy.

opment (Sluder *et al*., 1989). The centrosome, apart from organising the cytoskeleton, may pay a role in calcium signalling (Welsh *et al*., 1979; Wolniak *et al*., 1980; see Whitaker & Patel, 1990). In fact, pericentriolar material contains enzymes of the phosphoinositide metabolic pathway, suggesting a role in calcium release (Petzelt *et al*., 1989). Calcium increases and increased activity of calmodulin have been shown to be localised to the centrosomal region during mitosis (Wilding *et al*., 1996; Török *et al*., 1998), suggesting a physiological role for the centrosome in cell cycle calcium signalling.

In this paper, we examine the calcium transients produced in the ascidian *C. intestinalis* after fertilisation and compare the initiation of these transients with the position of the male centrosome. Our data show that ascidian sperm enter oocytes at the vegetal pole. Meiosis I-associated repetitive calcium waves originate from the vegetal pole of the oocyte, and progress towards the animal pole. However, meiosis II-associated waves traverse the oocyte cytoplasm through the equatorial region. The relocalisation of post-fertilisation calcium waves correlates highly with the relocalisation of the centrosome after meiosis I. We further demonstrate the presence of a calcium-induced calcium release (CICR) mechanism in unfertilised oocytes and demonstrate that this mechanism influences the speed of the calcium wave induced by injection of inositol 1,4,5-trisphosphate (IP_3) after fertilisation. Interestingly, parthenogenetic activation of ascidian oocytes by IP_3 or soluble sperm extracts did not lead to any increase in the velocity of the IP_3-induced calcium wave. These results suggest that the male centrosome influences both the site of initiation and the properties of post-fertilisation calcium waves, indicating that the role of this organelle in early development is more complex than that of focusing microtubule polymerisation.

Materials and methods

Collection and preparation of oocytes

Oocytes were dissected from the ascidian *Ciona intestinalis*, collected from the Bay of Naples and kept in tanks with running sea water until use. Oocytes were manually dechorionated using steel needles and placed in an injection chamber containing 2 ml natural filtered sea water (NSW) from the Bay of Naples. In some cases oocytes were enzymatically dechorionated in NSW containing 0.1% trypsin as previously described (McDougall & Sardet, 1995).

Microinjection and electrophysiological techniques

Standard patch pipettes of 2 μm diameter, 10 megaohm resistance were used for both microinjection and electrophysiology. Pipettes were backfilled with reagents dissolved in an intracellular solution (ICS) containing 200 mM K_2SO_4, 20 mM NaCl, 10 mM HEPES, pH 7.5 unless otherwise stated. After formation of a gigaohm seal, the patch was ruptured and reagents injected by pressure using an Eppendorf Transjector 5246 (the pressure injection system is required to introduce reagents into large cells such as ascidian oocytes). Injection volumes were estimated by measurement of the size of the pulse in the oocyte, measured by the displacement of cytoplasm after an injection at a controlled pressure. Control injections of up to 10% of oocyte volume of ICS did not affect oocytes. All reagents were obtained from Sigma except where stated.

Whole cell measurement of intracellular calcium

Calcium Green-1 dextran (10 000 M_r, Molecular Probes, OR) was dissolved in ICS and microinjected into oocytes to a concentration of 20 μg/ml. Calcium determinations were made by recording the fluorescence emission of Calcium Green-1 dextran after excitation through a 480 nm 10 nm FWHM excitation filter (Omega Optical). A 510 nm 20 nm FWHM filter was used to record fluorescent emission (Omega Optical). Data were recorded onto a microcomputer installed with CRS-400 electrophysiology/ion measurement software (BioRad). Fluorescence determinations were ratioed for comparison by dividing all emission intensities by the first point, defined as resting calcium.

Ratiometric confocal measurement of intracellular calcium

For ratiometric confocal calcium measurements, the calcium-sensitive dye Calcium Green-1 dextran (CGdx, 10 000 M_r, Molecular Probes) was used in conjunction with the calcium-insensitive dye tetramethylrhodamine dextran (TMRdx, 10 000 M_r, Molecular Probes) which reports cytoplasmic distribution (Gillot & Whitaker, 1993; McDougall & Sardet, 1995). These dyes were dissolved in ICS and co-injected. We determined that 5:1 CGdx:TMRdx was the best ratio in our system with minimum crosstalk between the two channels. Calcium determinations were made using an Olympus Fluoview confocal microscope system based on an Olympus IX-70 microscope and an Kr/Ar laser. Laser lines of 488 nm were used to excite CGdx and 568 nm for TMRdx. CGdx images were divided pixel-by-pixel by the TMRdx images to achieve a ratiometric image free of cytoplasmic distribution artefacts. The

https://doi.org/10.1017/S0967199400001088 Published online by Cambridge University Press

resulting image was then calibrated where necessary using previously established methods (Gillot & Whitaker, 1993).

Visualisation of tubulin

For fixing and tubulin visualisation, oocytes were dechorionated by trypsin treatment and samples fixed at defined times after fertilisation. Prior to fixation and extraction, oocytes were first washed into calcium-free artificial sea water (ASW) containing 500 mM NaCl, 10 mM KC1, 50 mM $MgSO_4$, 2.5 mM $NaHCO_3$, 10 mM EGTA, pH 8.0. Oocytes were then resuspended into a tubulin-stabilising extraction buffer containing 25% glycerol, 50 mM KC1, 50 mM imidazole-HC1 (pH 7.2), 0.5 mM MgCl2, 10 mM EGTA, 1 mM EDTA, 1 mM β-mercaptoethanol, 3% Triton X-100, 5% methanol. After 24 h of extraction, oocyte ghosts were attached to slides coated with 5 mg/ml poly-L-lysine and fixed in methanol at –10 °C for 6 min. Slides were then washed in phosphate-buffered saline (PBS) + 0.1% Triton X-100 for 5 min followed by PBS for 5 min. Slides were pre-treated with DNAse-free RNAse for 30 min at 37 °C to remove RNA followed by 5 min washes in PBS + 0.1% Triton X-100 and PBS. Slides were incubated in the dark for 1 h with an antibody to α-tubulin directly labelled with fluorescein. Slides were washed in the dark for 15 min with PBS + 0.1% Tween-20 followed by a 5 min wash with PBS. Propidium iodide (Molecular Probes) at 20 μg/ml in antifade solution (Electron Microscopy Sciences, Rome, Italy) was used to stain DNA. Confocal images were taken using an Olympus Fluoview confocal microscope system based on an Olympus IX-70 microscope and a Kr/Ar laser. Images were processed using Adobe Photoshop.

Sperm extract preparation

Ascidian sperm extracts were prepared according to previously published protocols (Wilding & Dale, 1998). Extracts were conserved at –80 °C, and injected into oocytes to 2–3 sperm-equivalents.

Results

Visualisation of male and female aster movements during meiosis

The ascidian oocyte is arrested prior to fertilisation during metaphase of meiosis I. Fertilisation therefore triggers the completion of both meiosis I and II before zygotes enter mitotic cleavage divisions. We used an antibody against α-tubulin to follow the movements of the male and female centresomal complexes in these oocytes after fertilisation. In unfertilised oocytes, the meiotic apparatus is clearly visible at the periphery of the oocyte with chromosomes in metaphase I. Just after fertilisation, the female meiotic apparatus is unchanged (Fig. 1a.i, left image) whereas the fertilising sperm forms a tubulin-containing 'fusion complex' at the vegetal pole of the oocyte (Fig. 1a.i, right image). As the oocyte completes meiosis I (Fig. 1a.ii, left image), the sperm centresome rapidly forms a centresomal complex at the vegetal pole of the oocyte (Fig. 1a.ii, right image). The meiotic apparatus does not fully degrade after the completion of meiosis I (Fig. 1a.iii, left image). Instead a 'half apparatus' persists in the interval between meiosis I and II (Fig. 1a.iii, left image). By 15 min after fertilisation, the meiotic apparatus has fully reformed (Fig. 1a.iv, left image). The second meiotic division has been completed by 20 min after fertilisation (Fig. 1a.v, left image). In contrast to the movements of the meiotic apparatus, the sperm centresome does not undergo further changes until meiosis is complete (Fig. 1a, right series).

It has been demonstrated previously that the sperm-derived centresome uniquely forms the mitotic apparatus in the sea urchin, whereas the female centresome breaks down after the completion of meiosis (Sluder *et al.*, 1989). Our data in ascidians confirm these findings. We noticed that the sperm centresome divided abruptly after the completion of meiosis to form the mitotic apparatus (Fig. 1b.i). We confirmed these data by observing the behaviour of maternal and paternal chromosomes in polyspermic oocytes. We noticed that polyspermy induced the formation of more than one mitotic aster (Fig. 1b.ii). However, only one free pronucleus was ever observed before pronuclear fusion (Fig. 1b.i, ii). Because the oocyte always contains only one set of chromosomes after the successful completion of meiosis, we attribute the extra copies of the mitotic apparatus to the penetration of more than one spermatozoon. The data therefore demonstrate that the male centresome uniquely forms the mitotic apparatus in ascidian zygotes, whereas the female meiotic centresome degenerates.

Calcium waves follow the position of the male centresome

We used a ratiometric confocal microscopy technique to determine the origin of the fertilisation calcium transient and repetitive post-fertilisation waves in ascidian oocytes. In 21 of 21 oocytes, the initial calcium transient that marked fertilisation propagated as a wave (Fig. 2a). The calculated velocity of the fertilisation wave is 6.9 ± 1.4 μM/s (mean ± SEM, n = 21; Fig. 2a, Table 1). The speed of progression of the fertilisation calcium wave in ascidians is equivalent to that of other species (Whitaker & Swann, 1993). Intracellular calcium measured by ratiometric confocal microscopy increased 2.4

https://doi.org/10.1017/S0967199400001088 Published online by Cambridge University Press

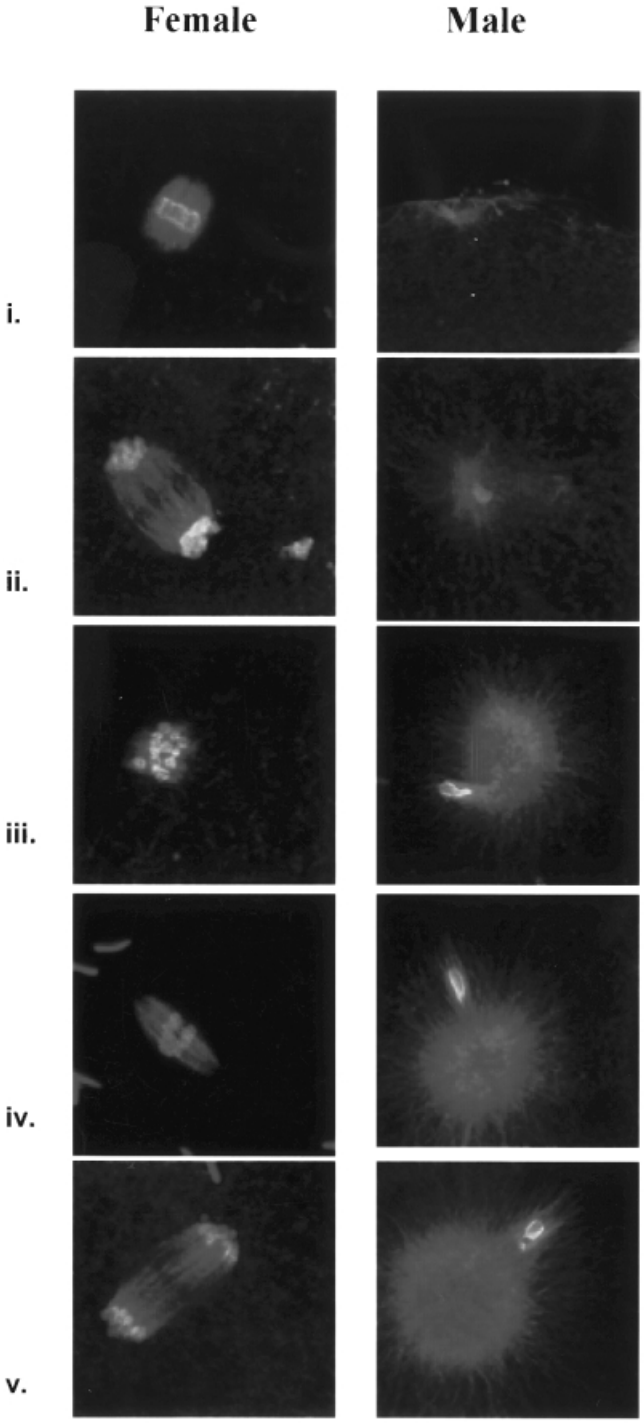

(a)

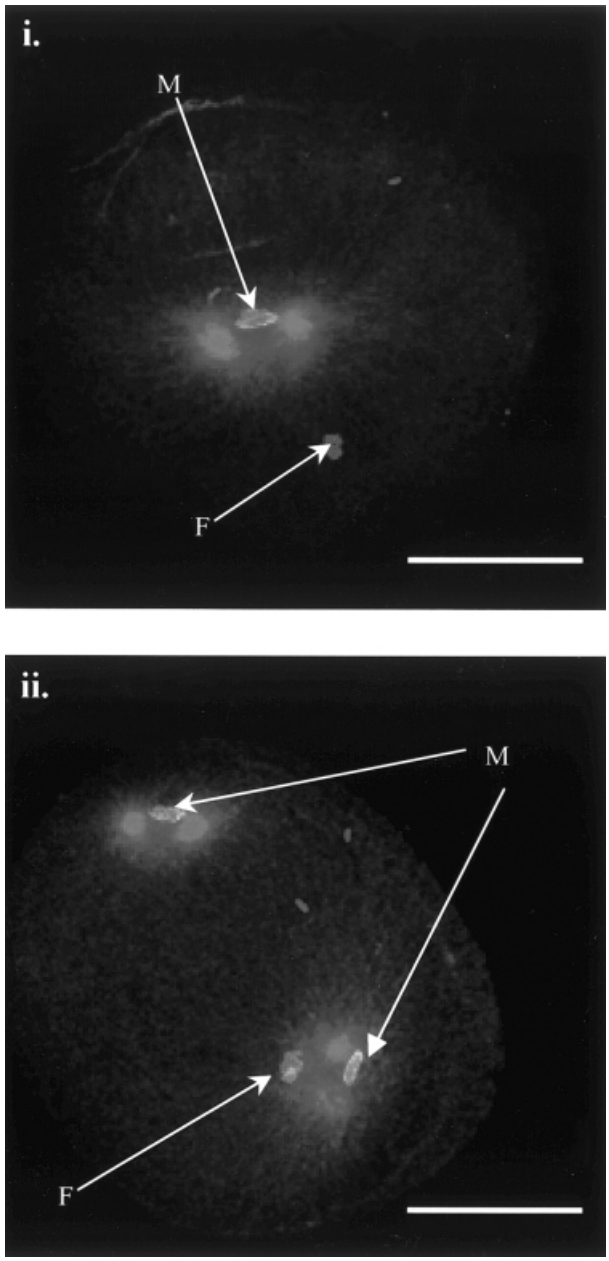

(b)

Figure 1 Localisation of tubulin reveals centrosome behaviour during meiosis. (*a*) Images show the formation and behaviour of male and female centrosomal complexes after fertilisation in *C. intestinalis*. Left, female; right, male. (i) At sperm addition; (ii) 5 min after fertilisation; (iii) 10 min after fertilisation; (iv) 15 min after fertilisation; (v) 25 min after fertilisation. A total of 5–10 images of separate oocytes were taken in six separate experiments. Times post-fertilisation represent timings after scoring of 50% contracted oocytes. Green represents microtubules, red represents chromatin. Scale bar represents 10 μm. (*b*) The male centrosome uniquely forms the meiotic apparatus. Oocytes were fixed 45 min after fertilisation. Green represents tubulin, red represents chromatin. Arrows: 'M', male pronucleus; 'F', female pronucleus. (i) A monospermic zygote undergoing pronuclear fusion; (ii) a polyspermic zygote undergoing pronuclear fusion. Note the presence of a pronucleus without attached centrosomal complex. This is the presumptive female pronucleus. Images are representative of 5–10 images taken from a total of six separate experiments. Scale bar represents 50 μm.

https://doi.org/10.1017/S0967199400001088 Published online by Cambridge University Press

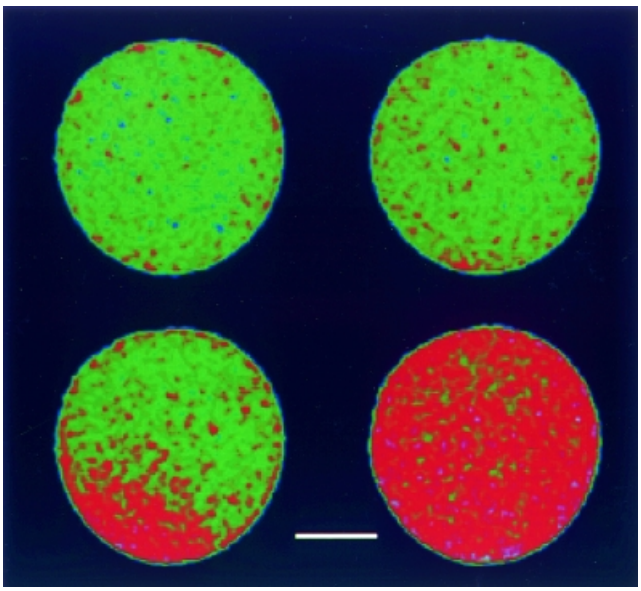

(a)

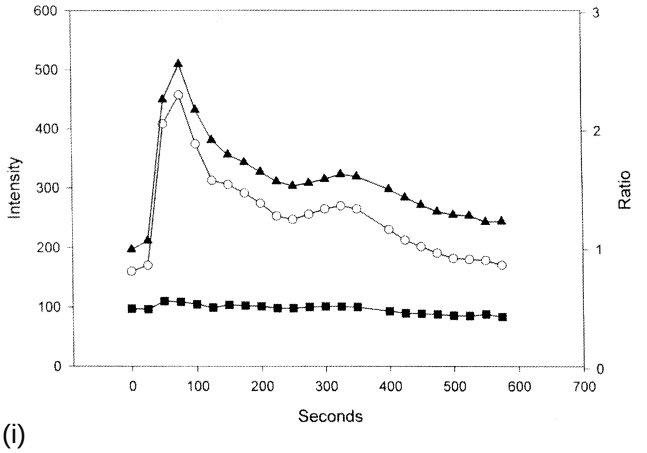

(i)

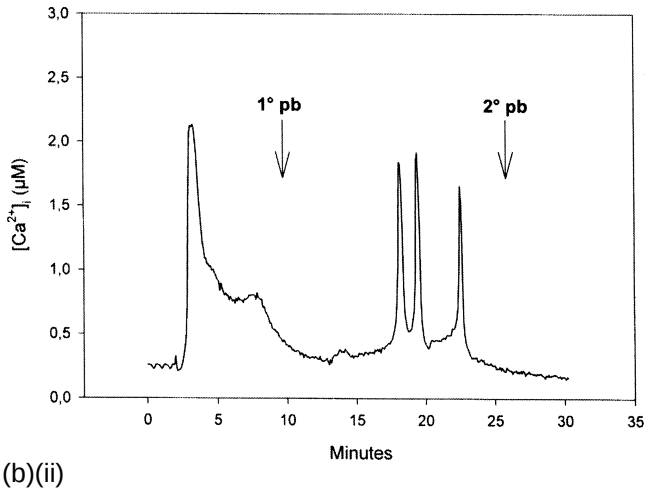

(b)(ii)

Figure 2 Ratiometric confocal imaging of calcium waves in ascidian oocytes. (*a*) Fertilisation calcium wave in *C. intestinalis*. The figure shows the ratioed result of the division pixel-by-pixel of images taken with Calcium Green-1 dextran (10 000 M_r, CGdx) by images of tetramethylrhodamine dextran (10 000 M_r, TMRdx) taken simultaneously from the same oocyte. A 5:1 ratio by concentration of CGdx to TMRdx was used (intracellular concentration: 20 μM CGdx to 4 μM TMRdx). The image is representative of 21 experiments. Images are presented in false colour, warmer colours representing higher calcium. The image is not calibrated for calcium levels. Images were taken at 6 s intervals. Scale bar represents 50 μm. (*b*) Calibration of confocal calcium trace. (i) Intensity plot of fertilisation calcium wave. Left axis ('Intensity') refers to raw intensity from the two channels. Black squares are intensity values for TMRdx and white circles intensity of CGdx. Right axis ('ratio') represents data obtained by dividing pixel-by-pixel the CGdx data by TMRdx data (black triangles). $n = 21$. (ii) Ratioed intensity data of calcium transients during meiosis in ascidian oocytes. The trace is calibrated for calcium by the method of Gillot & Whitaker (1993). $n = 15$.

± 0.2 μM above resting calcium (mean ± SEM, $n = 21$; Fig. 2b, Table 1), in agreement with previous observations using whole-cell calcium measurement (Wilding & Dale, 1998). The fertilisation wave was followed by a contraction of the cytoplasm, and emission of the first polar body.

By switching rapidly between fluorescence measurements and bright field observation, we were able to determine the position of the fertilisation calcium wave with respect to the emission of the first polar body. We noticed a strong correlation between the two events. Where the emission of the first polar body could be observed, the body was always emitted at an angle of 120–200° from the initiation of the fertilisation calcium wave ($n = 15$; Fig. 3, Table 1). Emission of the polar body was never observed at any other position relative to the fertilisation calcium wave in our experiments. These data agree with the localisation of the sperm-derived aster at fertilisation (see above), strongly suggesting that *C. intestinalis* sperm fuse with the oocyte in a specific region in the vegetal pole of the plasma membrane.

Ascidian oocytes are characterised by repetitive calcium waves that occur prior to the completion of meiosis I and II and terminate as the oocytes enter mitotic interphase (Speksnijder *et al.*, 1989; McDougall & Sardet, 1995; Russo *et al.*, 1996; McDougall & Levasseur, 1998). In our experiments, post-fertilisation

https://doi.org/10.1017/S0967199400001088 Published online by Cambridge University Press

Table 1 Properties of meiotic calcium transients

	Type of transient	Origin of transient	Wave speed (μm/s)	Calcium increase (μM)
Fertilisation (n = 21)	Wave	Vegetal pole	6.9 ± 1.4	2.4 ± 0.2
Metaphase I (n = 15)	Wave	Vegetal pole	14.6 ± 3.2*	1.5 ± 0.1
Metaphase II (n = 33)	Wave	Equator	15.8 ± 2.6*	1.6 ± 0.1

*Significantly faster than fertilisation wave, one tailed t-test $p < 0.001$.

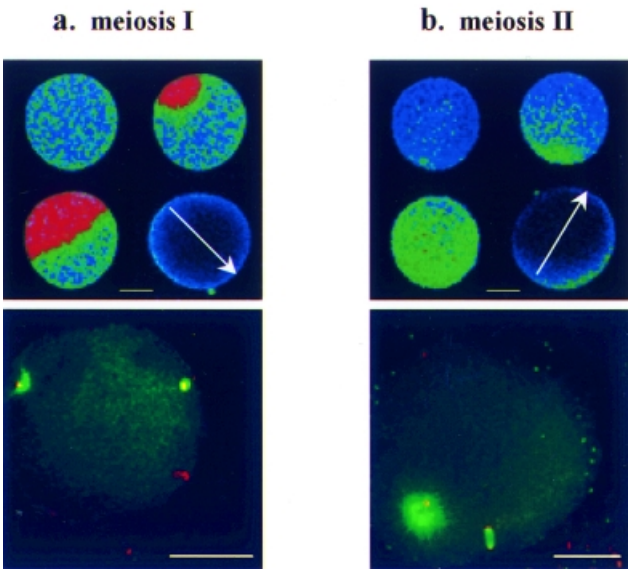

Figure 3 The origin of post-fertilisation calcium waves follows the localisation of the male centrosome. (*a*) Meiosis I; (*b*) meiosis II. Scale bar represents 50 μm for all images. Calcium waves are shown in 6 s intervals. Bottom right inserts in calcium images show the emission of the polar body (taken from raw data). Arrow describes the passage of the calcium waves through the oocyte prior to polar body emission. Images are in false colour, warmer colours representing higher intensity (n = 15). The position of the male and female centrosomes is shown underneath the calcium images. Images are taken from batch experiments and represent at least 30 images from 6 separate experiments.

calcium waves were observed in all experiments where fertilised oocytes completed meiosis (15/21, see Table 1). Meiosis I-associated calcium waves originated at the vegetal pole, and progressed towards the animal pole of the zygote (Fig. 3a, Table 1). In contrast, meiosis II-associated waves initiated in the equatorial region of the oocyte (Fig. 3b, Table 1). When oocytes were fixed and immunolocalised for tubulin, we noticed that the male centresome also lay in the equatorial region of the oocyte (n = 18).

The speed of IP_3-induced calcium waves increases after fertilisation, but not parthenogenetic activation

We have previously demonstrated that post-fertilisation calcium transients in ascidian oocytes are triggered by IP_3-induced calcium release (IICR; McDougal & Sardet, 1995; Russo *et al*., 1996; Wilding *et al*., 1997; Yoshida *et al*., 1998). However, more recent data suggest that calcium-induced calcium release (CICR) may modulate the repetitive calcium signal (Wilding *et al*., 1998). A CICR mechanism has been suggested to be

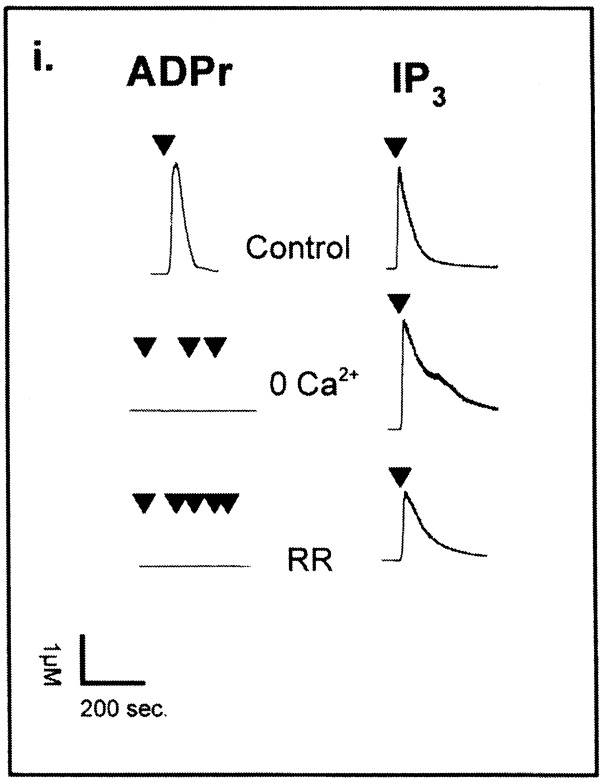

(i)

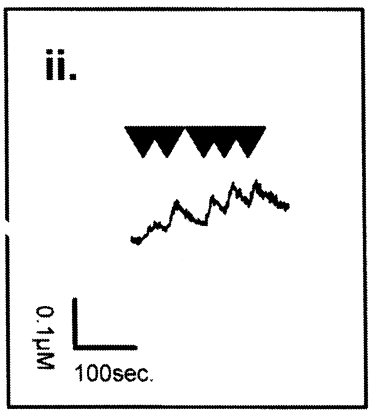

(ii)

Figure 4 (*a*) For legend see opposite

https://doi.org/10.1017/S0967199400001088 Published online by Cambridge University Press

present in ascidian oocytes (Wilding & Dale, 1998); however, the lack of any calcium-releasing effect of CICR agonists in ascidian oocytes (Ryanodine, cADPr; see Galione & Summerhill, 1996) has precluded a direct demonstration of CICR (Wilding *et al*., 1997; Wilding & Dale, 1998; Yoshida *et al*., 1998). Injection of ADPr into unfertilised oocytes gates a non-specific channel which causes an influx of extracellular calcium into the oocyte cytosol (Wilding *et al*., 1998). We used the calcium influx through the ADPr channel to test whether CICR was present in unfertilised oocytes. Injection of ADPr to an intracellular concentration of 1 μM triggered a calcium transient in unfertilised oocytes (Fig. 4a). This transient was blocked by preinjection of the CICR antagonist Ruthenium Red (Fig. 4a.i, ii). In contrast, IP_3-generated calcium transients were unaffected by preinjection of Ruthenium Red (Fig. 4a.i), demonstrating that the CICR-like calcium release mechanism is

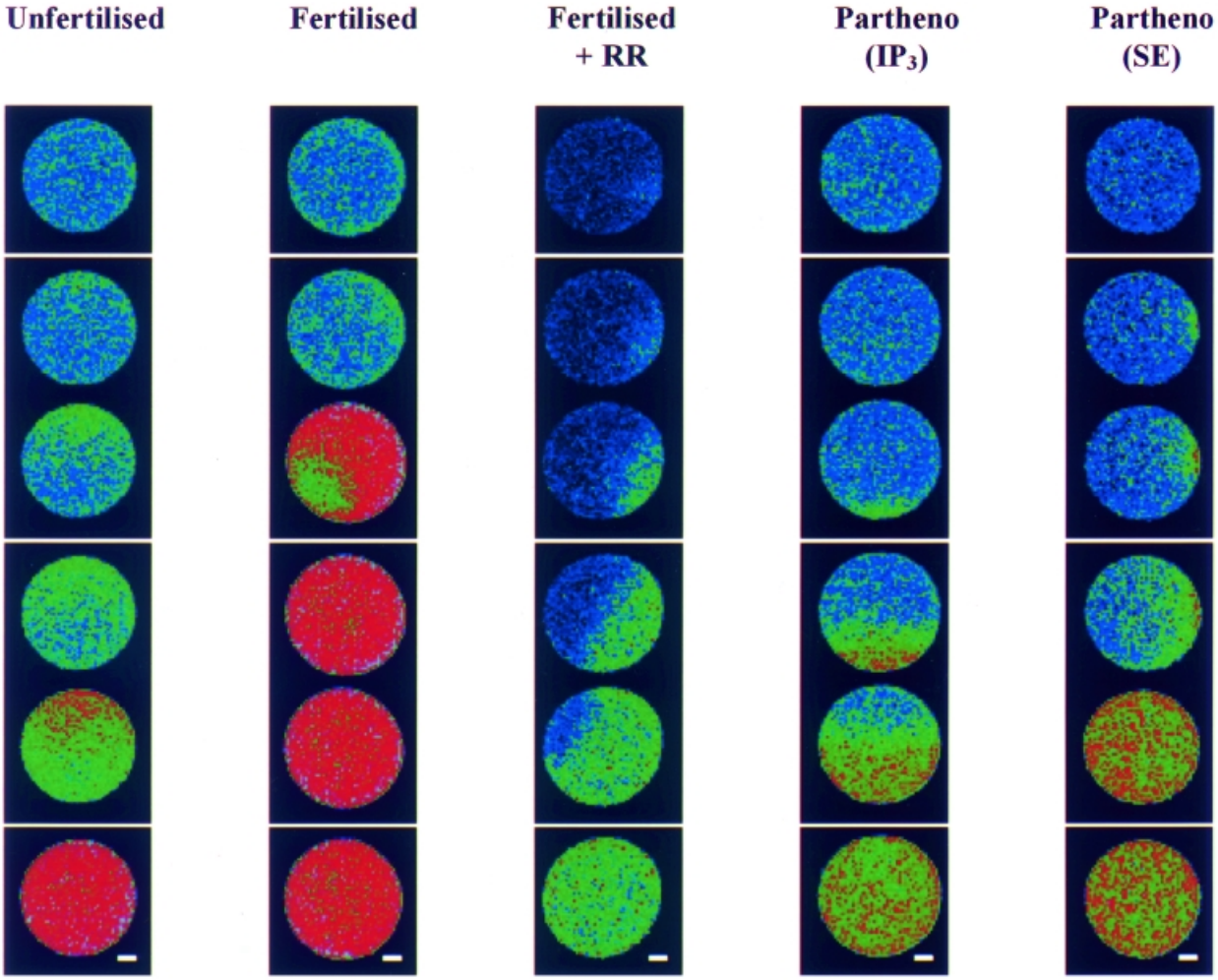

(b)

Figure 4 The speed of the IICR-induced calcium wave increases in fertilised oocytes. (*a*) Independent triggers of IICR and CICR in unfertilised oocytes. (i) ADPr (1 μM intracellular concentration) was used to trigger CICR. IP_3 (0.1 μM intracellular concentration) was used to trigger IICR. Top: Both ADPr and IICR trigger a calcium transient in unfertilised oocytes. n = 22 for both reagents. Centre: In calcium-free sea water (0 Ca^{2+}), IP_3 injection triggers an intracellular calcium transient whereas ADPr injection has no effect. n = 14 experiments for both reagents. Bottom: Oocytes were preinjected with the CICR inhibitor Ruthenium Red to 500 μM (Galione & Summerhill, 1996). n = 6 for both reagents. (ii) Expanded y-axis of an experiment of ADPr injection into Ruthenium-Red-treated oocytes. Small calcium transients are observed consistent with the influx of calcium ions through the ADPr channel (see Wilding *et al*., 1998). (*b*) IP_3-generated calcium waves in fertilised and parthenogenetically activated oocytes. IP_3 was injected to 0.1 μM intracellular concentration after various pretreatments. Images are in false colour at 5 s intervals. For statistics, see Table 2. Unfertilised: IP_3 injection into unfertilised oocytes (n = 13). Fertilised: IP_3 injection into oocytes 10 min after fertilisation (n = 8). Fertilised + RR: IP_3 injected into oocytes preinjected with Ruthenium Red to 500 μM and fertilised. Injections of IP_3 were 10 min after fertilisation (n = 6). Partheno (IP_3): IP_3 injected into oocytes parthenogenetically activated by prior injection of IP_3 (n = 12). Partheno (SE): IP_3 injected into oocytes 10 min after parthenogenetic activation by the injection of sperm extracts (n = 5). Scale bar represents 20 μm.

https://doi.org/10.1017/S0967199400001088 Published online by Cambridge University Press

independent of IICR in unfertilised oocytes. Post-fertilisation calcium waves in ascidian oocytes are triggered by an IP_3-dependent mechanism (McDougall & Sardet, 1995; Russo *et al*., 1996; Wilding *et al*., 1997). In the present experiments, we could not trigger CICR after fertilisation, supporting the above hypothesis (data not shown). Since the speed of repetitive post-fertilisation calcium waves in ascidian oocytes is significantly faster than the fertilisation wave (Table 2), we tested whether the speed the IICR-induced calcium wave changed after fertilisation. Injection of IP_3 into unfertilised ascidian oocytes triggers a calcium wave which progresses through the cytoplasm at a speed of 7.2 ± 2.2 μm/s (mean ± SEM, n = 13; Fig. 4b, Table 2). Injection of IP_3 after fertilisation triggered a faster calcium wave with a velocity of 15.1 ± 1.1 μm/s (mean ± SEM, n = 8; Fig. 4b, Table 2). The increase in wave speed measured after fertilisation was abolished when oocytes were preinjected with the CICR blocker Ruthenium Red, suggesting that CICR does play a role in post-fertilisation calcium waves (Fig. 4b, Table 2). Interestingly, repetitive injections of IP_3 into oocytes without exposure to sperm, or injections of IP_3 after activation of oocytes with soluble sperm extracts, did not lead to any significant alteration of the speed of the IP_3-induced calcium wave (Fig. 4b, Table 2). These data suggest that an insoluble component of sperm influences the mechanisms underlying the increase in speed of the calcium wave in fertilised oocytes.

Discussion

In this manuscript we have used ratiometric confocal calcium imaging and immunolocalisation of tubulin to define the movements of the male and female centrosomes after fertilisation and during meiosis and correlate these data with the localisation of meiosis-associated calcium waves.

Comparison of the initiation of the fertilisation wave in ascidians with the production of the first polar body suggests that ascidian sperm enter the oocyte at the vegetal pole. The data contradict previous findings in a related ascidian, *Phallusia mammilata* (Rogers *et al*., 1995), probably reflecting species differences. The fact that ascidian sperm can fuse and enter oocytes only at specific zones suggests either that the sperm receptor is localised to these zones, or that the vegetal pole exclusively permits sperm/egg fusion. After sperm/egg fusion, the sperm aster remains at the vegetal pole for the duration of meiosis I. During meiosis II, the sperm aster is found at the equator of the zygote. Using fixed oocytes, we could not determine whether the aster slowly changed position during meiosis I or abruptly moved during the transition to meiosis II; however, the fact that the male aster is found in the vegetal pole even up until the time the meiotic apparatus reforms prior to meiosis II suggests that the relocalisation of the aster occurs prior to the trigger of anaphase II.

Our data on the localisation of tubulin during meiosis reveal many differences between the oocyte- and sperm-derived centresomal complexes and chromatin. The sperm centresome quickly forms a large tubulin-containing complex after fertilisation. In contrast, the female centrosomal complexes remain small and underdeveloped. Our experiments furthermore demonstrate that the male aster uniquely divides to form the mitotic apparatus whereas the female asters degrade at the end of meiosis, as previously demonstrated (Sluder *et al*., 1989). In complete contrast, the male chromatin remains highly condensed during meiosis whereas the female chromatin is less condensed and female chromosomes are distinguishable. These data suggest that the physiology of the male and female centrosomes differ. The differences imply modes of regulation more complex than previous studies have suggested (Sluder *et al*., 1989). Our data suggest that a cytoplasmic factor inhibits the development of female centresomal complexes and causes these to degrade at the end of meiosis, whereas the sperm centrosome is protected against this factor. Interestingly, this factor appears to be protein synthesis dependent, because incubation of unfertilised ascidian oocytes in the presence of protein synthesis inhibitors caused the *de novo* formation of centrosomal complexes through-

Table 2 IP_3-induced calcium waves in fertilised and parthenogenetically activated oocytes

Type of activation	Pre-activation wave speed (μm/s)	Post-activation wave speed (IP_3, μm/s)
Fertilisation	7.2 ± 2.2 (n = 13)	15.1 ± 1.1 (n = 8)
Fertilisation + RR	7.0 ± 1.3 (n = 6)	6.1 ± 2.5 (n = 6)
Parthenogenesis (IP_3)	6.5 ± 1.3 (n = 12)	7.3 ± 1.3 (n = 12)
Parthenogenesis (SE)	7.2 ± 1.4 (n = 5)	6.9 ± 1.2 (n = 5)

RR, injection of Ruthenium Red to 500 μM intracellular concentration. Parthenogenesis (IP_3) was induced by the injection of IP_3 to 100 nM intracellular concentration. Parthenogenesis (SE) was induced through the injection of ascidian sperm extracts to 1% oocyte volume (Wilding & Dale, 1998).

https://doi.org/10.1017/S0967199400001088 Published online by Cambridge University Press

out the oocyte cytoplasm in the absence of sperm (Marino *et al*., 2000).

The properties of post-fertilisation calcium transients in ascidian oocytes suggest a strong influence by the male centrosome. In our experiments, the initiation site of post-fertilisation calcium transients was closely corrrelated with the localisation of the male aster throughout meiosis. In addition, we noted that parthenogenetic activation of ascidian oocytes by IP_3 or soluble extracts of ascidian spermatozoa did not cause any increase in the speed of later calcium waves triggered by IP_3 microinjection. These data suggest that components of spermatozoa not retained in the soluble extract are involved in influencing the properties of IP_3-induced calcium release post-fertilisation. At fertilisation, the spermatozoon introduces two major insoluble components: the nucleus and the centrosome. It is therefore feasible to hypothesise that the sperm centrosome is involved in the alteration of the properties of IICR in the oocyte. The fact that the speed of post-fertilisation calcium waves is sensitive to Ruthenium Red further suggests that the mechanism involves an alteration of the properties of the oocyte to CICR.

Acknowledgement

We thank Giuseppe Gargiulo for his technical help during this work.

References

Dale, B., DeFelice, L.J. & Ehrenstein G. (1985). Injection of a soluble sperm extract into sea urchin eggs triggers the cortical reaction. *Experientia*, **41**, 1068–70.

Dale, B., Marino, M. & Wilding, M. (1999). Sperm-induced calcium oscillations: soluble factor, receptor, or receptors? *Mol. Hum. Reprod.* **5**, 1–4.

Galione, A. & Summerhill, R. (1996). Regulation of ryanodine receptors by cyclic ADP-ribose. In *Ryanodine Receptors*, ed. V. Sorrentino, pp. 52–70. Boca Raton: CRC Press.

Gillot, I. & Whitaker, M. (1993). Imaging calcium waves in eggs and embryos. *J. Exp. Biol*. **184**, 213–19.

Jaffe, L.F. (1980). Calcium explosions as triggers of development. *Ann NY Acad. Sci.* **339**, 86–101.

Marino, M., Wilding, M. & Dale, B. (2000). Interaction of cell cycle kinases, microtubules and chromatin in ascidian oocytes during meiosis. *Mol. Reprod. Dev.* **56**, 155–62.

McDougall, A. & Levasseur, M. (1998). Sperm-triggered calcium oscillations during meiosis in ascidian oocytes first pause, restart, then stop: correlations with cell cycle kinase activity. *Development* **125**, 4451–4459.

McDougall, A. & Sardet, C. (1995). Function and characteristics of repetitive calcium waves associated with meiosis. *Curr. Biol.* **5**, 318–328.

Petzelt, C., Joswig, G. & Batz, A. (1989). Where in the hierarchy stands the centresome in intracellular calcium regulation? *Eur. J. Cell Biol.* **48** (Suppl 26), 29.

Rogers, F., McDougall, A. & Sardet, C. (1995). The sperm entry point defines the orientation of the calcium-induced contraction wave that directs the first phase of cytoplasmic reorganisation in the ascidian egg. *Development* **121**, 3457–66.

Russo, G.L., Kyozuka, K., Antonazzo, L., Tosti, E. & Dale, B. (1996). Maturation promoting factor in ascidian oocytes is regulated by different intracellular signals at meiosis I and II. *Development* **122**, 1995–2003.

Sluder, G. & Reider, C.L. (1985). Experimental separation of pronuclei in fertilised sea urchin eggs: chromosomes do not organise a spindle in the absence of centrosomes. *J. Cell Biol.* **100**, 897–903.

Sluder, G., Miller, F.J., Lewis, K., Davison, E.D. & Rieder, C.L. (1989). Centrosome inheritance in starfish zygotes: selective loss of the maternal centrosome after fertilisation. *Dev. Biol.* **131**, 567–579.

Speksnijder, A., Corson, D., Sardet, C. & Jaffe, L. (1989). Free calcium pulses following fertilisation in the ascidian egg. *Dev. Biol.* **135**, 182–90.

Speksnijder, J. (1992). The repetitive calcium waves in the fertilised ascidian egg are initiated near the vegetal pole by a cortical pacemaker. *Dev. Biol.* **153**, 259–71.

Torok, K., Wilding, M., Groigno, L., Patel, R. & Whitaker, M. (1998). Imaging the spatial dynamics of calmodulin activity during meiosis. *Curr. Biol.* **8**, 692–9.

Welsh, M.J., Dedman, J.R., Brinkley, B.R. & Means, A.R. (1979). Tubulin and calmodulin: effects of microtubule and microfilament inhibitors on localisation in the mitotic apparatus. *J. Cell Biol.* **81**, 624–34.

Whitaker, M. & Patel, R. (1990). Calcium and cell cycle control. *Development* **108**, 525–42.

Whitaker, M. & Swann, K. (1993). Lighting the fuse at fertilisation. *Development* **117**, 1–12.

Wilding, M. & Dale, B. (1998). Soluble extracts of ascidian spermatozoa trigger intracellular calcium release independently of the activation of the ADP-ribose channel. *Zygote* **6**, 149–54.

Wilding, M., Wright, E., Patel, R., Ellis-Davies, G. & Whitaker, M. (1996). Local perinuclear calcium signals associated with mitosis entry in early sea urchin embryos. *J. Cell Biol*. **135**, 191–9.

Wilding, M., Kyozuka, K., Russo, G.L., Tosti, E. & Dale, B. (1997). A soluble extract from human spermatozoa activates ascidian oocytes. *Dev. Growth Differ.* **39**, 329–36.

Wilding, M., Russo, G., Marino, M. & Dale, B. (1998). ADP ribose gates the fertilisation channel in ascidian oocytes. *Am. J. Physiol.* **275**, C1277–83.

Wilson, E.B. & Matthews, A. (1895). Maturation, fertilisation and polarity in the echinoderm egg. *J. Morphol.* **10**, 319–42.

Wolniak, S.M., Hepler, P.K. & Jackson, W.T. (1980). Detection of the membrane calcium distribution during mitosis in *Haemanthus* endosperm with chlortetracycline. *J. Cell Biol.* **87**, 23–32.

Yoshida, M., Sensui, N., Inoue, T., Morisawa, M. & Mikoshiba, K. (1998). Role of two series of calcium oscillations in activation of ascidian eggs. *Dev. Biol.* **203**, 122–33.